

Phase diagram of ultrathin Pb (Zr 0.5 Ti 0.5) O 3 films under strain

Zhongqing Wu, Ningdong Huang, Jian Wu, Wenhui Duan, and Bing-Lin Gu

Citation: [Applied Physics Letters](#) **86**, 202903 (2005); doi: 10.1063/1.1929868

View online: <http://dx.doi.org/10.1063/1.1929868>

View Table of Contents: <http://scitation.aip.org/content/aip/journal/apl/86/20?ver=pdfcov>

Published by the [AIP Publishing](#)

Articles you may be interested in

[Domain structure sequence in ferroelectric Pb \(Zr 0.2 Ti 0.8 \) O 3 thin film on MgO](#)

Appl. Phys. Lett. **90**, 162906 (2007); 10.1063/1.2727563

[Ferroelectric domains and piezoelectricity in monocrystalline Pb \(Zr , Ti \) O 3 nanowires](#)

Appl. Phys. Lett. **90**, 133107 (2007); 10.1063/1.2716842

[Temperature-strain phase diagram for Ba Ti O 3 thin films](#)

Appl. Phys. Lett. **88**, 072905 (2006); 10.1063/1.2172744

[Electric-field-induced orthorhombic phase in Pb \[\(Zn 1 3 Nb 2 3 \) 0.955 Ti 0.045 \] O 3 single crystals](#)

J. Appl. Phys. **97**, 044105 (2005); 10.1063/1.1849819

[Piezoelectric performances of lead-reduced \(1 - x \) \(Bi 0.9 La 0.1 \) \(Ga 0.05 Fe 0.95 \) O 3 - x \(Pb 0.9 Ba 0.1 \) Ti O 3 crystalline solutions in the morphotropic phase boundary](#)

J. Appl. Phys. **96**, 6611 (2004); 10.1063/1.1810633

Agilent's Electronic Measurement Group is becoming **Keysight Technologies**.



Engineering Education & Research Resources DVD 2014

Agilent is the key to your test and measurement needs **Order yours**



Phase diagram of ultrathin $\text{Pb}(\text{Zr}_{0.5}\text{Ti}_{0.5})\text{O}_3$ films under strain

Zhongqing Wu, Ningdong Huang, Jian Wu, Wenhui Duan,^{a)} and Bing-Lin Gu
Center for Advanced Study and Department of Physics, Tsinghua University, Beijing 100084,
People's Republic of China

(Received 30 November 2004; accepted 4 April 2005; published online 10 May 2005)

Using a first-principles-based approach, we investigate the strain–temperature phase diagram of $\text{Pb}(\text{Zr}_{0.5}\text{Ti}_{0.5})\text{O}_3$ ultrathin film without surface charge screening. We find that the compressive strain dramatically affects the sequence of phase transitions, and observe a rich variety of ferroelectric phases, including a monoclinic phase and a stripe domain forbidden in the bulk crystal. The vortex stripe structure leads to an unusual characteristic of the phase diagram. © 2005 American Institute of Physics. [DOI: 10.1063/1.1929868]

During the past decade, ferroelectric thin films has been extensively investigated due to their physical properties and their promising applications in microelectronics such as non-volatile random access memories.^{1–3} Many experimental works reveal that the physical properties of the film are distinctly different from those of bulk materials. An important factor influencing the film properties is the strain resulting from lattice mismatching between the film and substrate since the polarization is strongly coupled to strain.⁴ The theoretical studies demonstrated that the strain can change the sequence of the phase transitions and induce the phases forbidden in bulk material.^{5–7} However, in these works, only films with thickness much larger than the ferroelectric correlation length are considered, and the short-circuit electrical boundary conditions are imposed. The effect of the strain on the ultrathin film (only a few nanometers thick) without any charge screening still have not been investigated in depth. In fact, the ultrathin film may exhibit more complex behavior when no charge screening is introduced (namely, the effect of a depolarization field is considered). For example, an unusual atomic off-center displacement vortex pattern in BaTiO_3 quantum dots⁸ and stripes in $\text{Pb}(\text{Zr}_{0.5}\text{Ti}_{0.5})\text{O}_3$ (Refs. 9–11) were observed very recently. How these polarization patterns remarkably influence the film properties should be a very interesting issue.

In this letter, we investigate the effects of the strain on the properties of disorder $\text{Pb}(\text{Zr}_{0.5}\text{Ti}_{0.5})\text{O}_3$ ultrathin films by use of Monte Carlo simulations. We adopt the effective Hamiltonian of $\text{Pb}(\text{Zr}_{1-x}\text{Ti}_x)\text{O}_3$ (PZT) alloys proposed by Bellaiche *et al.*,¹² which is derived from first-principles calculations. The above-mentioned approach can provide microscopic information about the atomic off-center displacements and therefore is especially fit to investigate the film without any charge screening, where the unusual polarization pattern may be formed. The effective Hamiltonian are represented by a low-order Taylor expansion of the relevant variables: soft mode and strain, since the ferroelectric phase transition involves only very small atomic displacements and strain deformations from the high-symmetric cubic structure. For PZT alloys, compositional degrees of freedom should be included in the effective Hamiltonian. Therefore, the total energy E is written as the sum of average energy and local energy as^{12,13}

$$E(\{\mathbf{u}_i\}, \{\mathbf{v}_i\}, \eta_H, \{\sigma_j\}) = E_{\text{ave}}(\{\mathbf{u}_i\}, \{\mathbf{v}_i\}, \eta_H) + E_{\text{loc}}(\{\mathbf{u}_i\}, \{\mathbf{v}_i\}, \{\sigma_j\}), \quad (1)$$

where \mathbf{u}_i is the local soft mode in the i th unit cell, \mathbf{v}_i is the dimensionless local displacement related to the inhomogeneous strain,¹⁴ η_H is the homogeneous strain tensor, and $\sigma_j = \pm 1$ represents the presence of a Zr or Ti atom at the j th lattice site of the PZT alloy. All the parameters of the Hamiltonian are derived from the first principles calculations and are listed in Refs. 12,13. While simulating nanoscopic structures, we do not include an external term of surface effect proposed by Fu and Bellaiche, since they demonstrated that the term has almost no effect on the polarization pattern.^{8,15}

In our simulations, the film is surrounded by vacuum. To efficiently calculate the long-range dipole–dipole interaction energy in thin films that lack the periodicity in the out-of-plane direction, we adopt the corrected three-dimensional Ewald method, whose validity has been verified analytically by Bródka and Grzybowski.¹⁶

From the previous Hamiltonian, Monte Carlo simulations are conducted. The details of the simulation process can be found in Ref. 9. The supercell average of the soft modes is directly proportional to the macroscopic electrical polarization. The influence of the substrate is imposed by confining the homogeneous in-plane strain. Namely, $\eta_1 = \eta_2 = \eta$ and $\eta_6 = 0$. The z axis ([001] direction) lies along the growth direction of the film, and the x and y axes are chosen to be along the pseudocubic [100] and [010] directions. The temperature is rescaled due to the fact that the effective-Hamiltonian approach overestimates the phase transition temperature.¹² The simulation temperature of 30 K corresponds to a rescaled experimental temperature of 18 K.

We find that the supercell average value of the out-of-plane local mode always remains at zero at any compressive strain. This is consistent with the boundary condition that film is surrounded by vacuum and no any charge screening is introduced. Our previous works demonstrated that the local mode displacements form a vortex stripe structure at large compressive strain.¹⁰ A feature of this vortex stripe is that the local mode displacement along the vortex stripe in any unit cell can be overlooked. Here we observe another kind of vortex structure shown in Fig. 1, where the local mode displacements along the vortex stripe (namely, the x direction) are considerably large in any unit cell and are in the same direction. For simplicity, we denote the former vortex stripe domain as “stripe domain A” and the latter as “stripe domain B.” The vortex stripe leads to the the spatial oscillation of the

^{a)} Author to whom correspondence should be addressed.

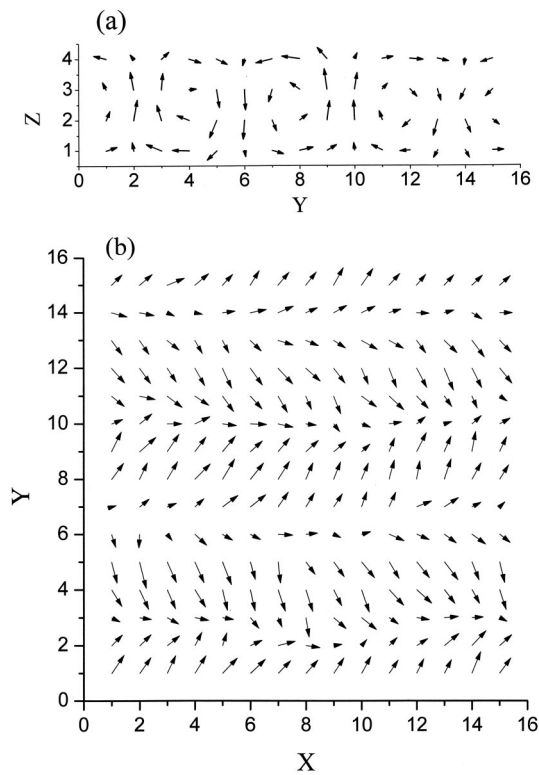


FIG. 1. Local-mode displacement, \mathbf{u}_i , of the cell in (a) $x=8$ plane and (b) $z=1$ plane of $15 \times 15 \times 4$ supercell under 1.6% compressive strain. The arrows give the directions of these displacements, projected on corresponding planes. The arrow length indicates the projected magnitude.

out-of-plane polarization. Therefore it should be appropriate to denote the out-of-plane polarization of the film by the modulation amplitude (Δu_z) of periodic stripe domains. Meanwhile, the in-plane polarization is denoted by the supercell average (u_x, u_y) of the in-plane local soft modes.

The temperature-strain phase diagram is presented in Fig. 2. The strain drastically affects the phase transition sequence. The phase diagram is divided into the following five parts by lines 1 (solid square), 2 (solid triangle), and 3 (open triangle): (i) C-type monoclinic (M_c) phase, where $u_x > u_y \neq 0$ and $\Delta u_z = 0$; (ii) orthorhombic (O) phase, where $u_x \neq 0$ and $u_y = \Delta u_z = 0$; (iii) stripe domain B (S_b), where $u_x \neq 0$; (iv) stripe domain A (S_a); and (v) paraelectric (P) phase. The appearance of the vortex structures leads to the spatial variation of the out-of-plane polarization and the formation of the stripe domain. In the S_a phase, the vortex stripes are responsible for the 180° domains observed. However in the S_b phase, owing to $u_x \neq 0$, the stripe domains are not 180° but approximately $2 \arctan(\Delta u_z / u_x)$, which depends on the strain or temperature of the S_b phase.

As the strain increases, the phase transition temperatures of M_c - O and O - P transitions increase, whereas the phase transition temperatures of S_b - M_c , S_b - O , and S_a - P transitions decrease. This indicates that the compressive strain suppresses the in-plane polarization and supports the out-of-plane polarization. The temperature region of the vortex stripe domain increases with the compressive strain. It is obvious that the compressive strain can stabilize the stripe domain. Note that the M_c and S_b phases do not exist in bulk PZT. Thus, the reduction of dimensionality induces phases forbidden in bulk.

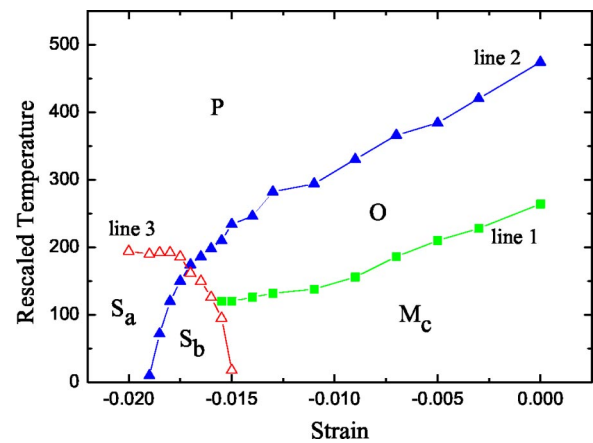


FIG. 2. The phase diagram of $\text{PbZr}_{0.5}\text{Ti}_{0.5}\text{O}_3$ film. The film thickness is of four unit cells. The phase diagram are divided into the following five parts by lines 1 (solid square), 2 (solid triangle), and 3 (open triangle).

The above-mentioned phase diagram is different from those reported in the BaTiO_3 (Ref. 6) and PbTiO_3 (Ref. 5) thin films. One difference is embodied in the pattern of the z -direction polarization, which results from the different electrical boundary condition. In Refs. 6 and 5, the z -direction polarization monodomain is formed in the film because the short-circuit electrical boundary conditions are imposed. On the contrary, due to the open circuit electrical boundary conditions in our simulation, the z -direction polarizations form stripe domains in order to reduce the depolarization field energy. The vortex-like polarization pattern of the stripe further influences the phase diagram character, which will be discussed in the following in detail. Another difference is embodied in the phases with in-plane polarization. For $\text{Pb}(\text{Zr}_{0.5}\text{Ti}_{0.5})\text{O}_3$ ultrathin films, the phases with in-plane polarization are M_c and O phase. However, the phase with in-plane polarization exhibits the polarization of $u_x = u_y$ in BaTiO_3 and PbTiO_3 thin films, which is named as “aa-phase” in Ref. 5. The difference should be closely related to the fact that the $\text{Pb}(\text{Zr}_{0.5}\text{Ti}_{0.5})\text{O}_3$ is nearby the morphotropic phase boundary of $\text{Pb}(\text{Zr}_{1-x}\text{Ti}_x)\text{O}_3$. The M_c to O phase transition in $\text{Pb}(\text{Zr}_{0.5}\text{Ti}_{0.5})\text{O}_3$ ultrathin films is very similar to the monoclinic-to-tetragonal phase transition that bulk $\text{Pb}(\text{Zr}_{1-x}\text{Ti}_x)\text{O}_3$ undergoes in the morphotropic phase boundary. Interestingly, we found that the aa-phase is stable if we do not fix η_6 (namely let η_6 vary freely in the simulation) as done in Ref. 9. This indicates that the in-plane shearing strain η_6 also has important influence on the phase diagram.

The phase diagram exhibits an unusual character. In contrary to line 2, line 1 does not extend into the vortex stripe (see Fig. 2). This is closely related to the character of the vortex stripe. Besides the formation of the out-of-plane polarization stripe, the vortex character implies that the supercell average of the local mode normal to the stripe must be zero although the local modes normal to the stripes in any cell are considerably large. In our simulations, the vortex stripe is normal to the y axis. Thus the appearance of the stripe ($\Delta u_z \neq 0$) must go along with $u_y = 0$, which leads to that line 1 does not extend into S_b region.

Figures 3(a) and 3(b) show the sequence of phase transition at fixed strain ($\eta = -0.0155$) and at fixed temperature ($T = 18$ K), respectively. At $\eta = -0.0155$, the film exhibits S_b phase at low temperature. As the temperature increases, the film undergoes respectively three phase transitions: S_b - M_c ,

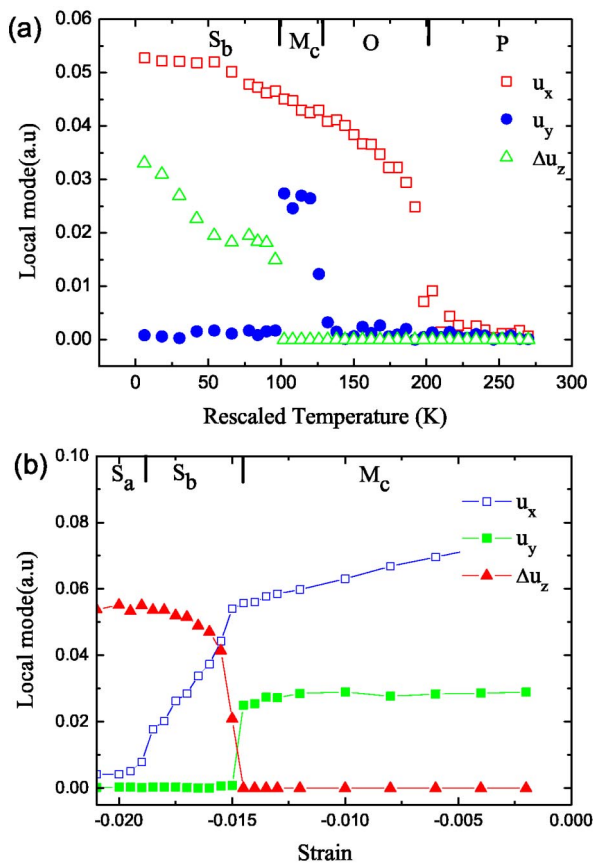


FIG. 3. The supercell average (u_x, u_y) of local mode, and the average amplitude Δu_z of the spatial variation in out-plane local mode (a) as a function of temperature under 1.55% compressive strain, and (b) as a function of strain at rescaled temperature 18 K.

M_c – O , and O – P transitions. At $T=18$ K, as the strain increases, the film undergoes respectively two phase transitions: S_a – S_b , and S_b – M_c transitions. Figure 3 clearly indicates that Δu_z and u_y cannot coexist. u_y must be null when $\Delta u_z \neq 0$, which denotes the appearance of the vortex stripe. The appearance of the vortex stripe is very abrupt, which indicates that the phase transition is of first order. Similar phenomena can also be observed in film under free in-plane shear strain η_6 .⁹

Figure 4 shows how the film thickness influences the critical strains for the M_c – S_b and S_b – S_a phase transitions.

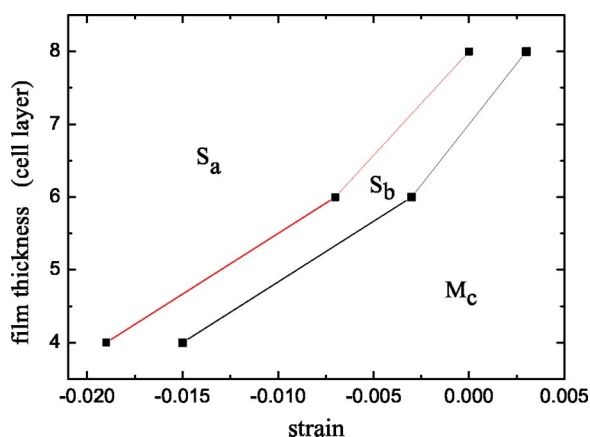


FIG. 4. The dependence of the critical strain for M_c – S_b and S_b – S_a phase transitions on the film thickness.

Both critical strains increase with increasing thickness. This can be easily understood from the fact that the out-of-plane long-range dipole interaction is enhanced with increasing film thickness. When the thickness is larger than seven unit cells, the vortex stripe S_b with significant z -direction polarization component can even exist in tensile strain. Similar polarization feature was also reported in BaTiO_3 (Ref. 6) and PbTiO_3 (Ref. 5) films, where the phase with polarization $P_x = P_y \neq 0$, $P_z \neq 0$ was found to be stable for thicker films in tensile strain. Our result indicates a possibility that the phase with $P_x = P_y = 0$, $P_z \neq 0$ (corresponding to “c phase” in Ref. 5) might also exist in tensile strain for ultrathin films with certain thicknesses (about ten unit cells). However, this conclusion might not be valid for the film with a larger thickness, as reported in BaTiO_3 (Ref. 6) and PbTiO_3 (Ref. 5) films with thicknesses larger than 50 nm. It is worthwhile performing further studies of the phase structure of the films with intermediate thickness.

In summary, the compressive strain–temperature phase diagram of ultrathin PZT film has been constructed with the Monte Carlo simulations based on a first-principle-derived Hamiltonian. The strain drastically affects the ferroelectric properties of film. A rich variety of ferroelectric phases are found, including a C-type monoclinic phases and a vortex stripe domain S_b , forbidden in the bulk crystal, which indicates an essential difference between ultrathin films and bulk crystals. The distinction between S_a and S_b is that the local mode displacements along the vortex stripe are considerably large in S_b phase but can be overlooked in the S_a phase. The vortex pattern leads to the unusual characteristics of the phase diagram: line 1 in Fig. 2 does not extend into the vortex phase and an expected new phase does not appear.

This work was supported by the State Key Program of Basic Research Development of China (Grant No. TG2000067108), the National Natural Science Foundation of China (Grant Nos. 10325415 and 50432030), and the China Postdoctoral Science Foundation.

¹J. F. Scott and C. A. Araujo, *Science* **246**, 1400 (1989).

²R. Waser and A. Rüdiger, *Nat. Mater.* **3**, 82 (2004).

³C. H. Ahn, Th. Tybell, and J.-M. Triscone, *Science* **303**, 488 (2004).

⁴R. E. Cohen, *Nature (London)* **358**, 136 (1992).

⁵N. A. Pertsev, A. G. Zembilgotov, and A. K. Tagantsev, *Phys. Rev. Lett.* **80**, 1988 (1998).

⁶O. Diéguez, S. Tinte, A. Antons, C. Bungaro, J. B. Neaton, K. M. Rabe, and D. Vanderbilt, *Phys. Rev. B* **69**, 212101 (2004).

⁷Y. L. Li, S. Choudhury, Z. K. Liu, and L. Q. Chen, *Appl. Phys. Lett.* **83**, 1608 (2003).

⁸H. Fu and L. Bellaiche, *Phys. Rev. Lett.* **91**, 257601 (2003).

⁹Z. Q. Wu, N. D. Huang, Z. R. Liu, J. Wu, W. H. Duan, B. L. Gu, and X. W. Zhang, *Phys. Rev. B* **70**, 104108 (2004).

¹⁰Z. Q. Wu, N. D. Huang, Z. R. Liu, J. Wu, W. H. Duan, and B. L. Gu, *arXiv: cond-mat/0407686*

¹¹S. K. Streiffer, J. A. Eastman, D. D. Fong, C. Thompson, A. Munkholm, M. V. R. Murty, O. Auciello, G. R. Bai, and G. B. Stephenson, *Phys. Rev. Lett.* **89**, 067601 (2002).

¹²L. Bellaiche, A. Garcia, and D. Vanderbilt, *Phys. Rev. Lett.* **84**, 5427 (2000).

¹³L. Bellaiche, A. Garcia, and D. Vanderbilt, *Ferroelectrics* **266**, 41 (2002).

¹⁴W. Zhong, D. Vanderbilt, and K. M. Rabe, *Phys. Rev. Lett.* **73**, 1861 (1994); *Phys. Rev. B* **52**, 6301 (1995).

¹⁵Although the above effective Hamiltonian was developed for bulk PZT, the surface effect is partially and implicitly considered during the simulations on the films by (i) including the effect of the broken bonds in the surfaces, which is substantial for the surface energy; and by (ii) relaxing the local soft mode vectors and inhomogeneous strain, which partially reflects the effect of surface relaxation.

¹⁶A. Bródka and A. Grzybowski, *J. Chem. Phys.* **117**, 8208 (2002).